Research Paper
Computational Methods for Differential Equations
http://cmde.tabrizu.ac.ir
Vol. *, No. *, *, pp. 1-21
DOI:10.22034/cmde.2024.54090.2265

A method of lines for solving the nonlinear time- and space-fractional SchrÖdinger equation via stable Gaussian radial basis function interpolation

Behnam Sepehrian* **and Zahra Shamohammadi**

Department of Mathematics, Faculty of Science, Arak University, Arak 38156-8-8349, Iran.

Abstract

The stable Gaussian radial basis function (RBF) interpolation is applied to solve the time- and space-fractional Schrödinger equation (TSFSE) in one and two dimensional cases. In this regard, the fractional derivatives of stable Gaussian radial basis function interpolants are obtained. By a method of lines the computations of the TSFSE are converted to a coupled system of Caputo fractional ODEs. To solve the resulted system of ODEs, a high order finite difference method is proposed, and the computations are reduced to a coupled system of nonlinear algebraic equations, in each time step. Numerical illustrations are performed to certify the ability and accuracy of the new method. Some comparisons are made with the results in other literature.

Keywords. Caputo derivative, Nonlinear, Fractional Schrödinger equation, Radial basis functions, Riesz derivative.
2010 Mathematics Subject Classification. 35G16, 65N06.

1. Introduction

One of the widely used models in mathematical physics is Schrödinger equation that appears in various disciplines such as plasma physics, nonlinear optics, quantum mechanics, dynamics of accelerators, fluid dynamics, and many other fields. The standard (non-fractional) Schrödinger equation was derived by using the Feynman path integral technique based on the Gaussian probability distribution in the space of all possible paths [8, 30]. In other words, in quantum mechanics, the Schrödinger equation are used to investigate the classical Brownian motion. Laskin extended the Feynman path integral to Lévy one, and introduced the Riesz space-fractional Schrödinger equation [14, 15]. In quantum physics, the Caputo time-fractional Schrödinger equation was applied to model the non-Markovian evolution [12, 21, 29]. Wang and Xu [34] considered the backgrounds of Laskin's and Naber's works and introduced the time- and space- fractional Schrödinger equation (TSFSE).
In the current paper, we consider the nonlinear TSFSE as follows: [13, 19]

$$i\,{}^{c}D_{t}^{\alpha}\psi(x,t)+\eta\frac{\partial^{\gamma}\psi(x,t)}{\partial|x|^{\gamma}}+q|\psi(x,t)|^{2}\psi(x,t)=f(x,t),\ a\le x\le b, \tag{1.1}$$

with the initial condition

$$\psi(x,0)=g(x),\ a\le x\le b, \tag{1.2}$$

and boundary conditions

$$\psi(a,t)=h_1(t),\ 0<t\le T, \tag{1.3}$$
$$\psi(b,t)=h_2(t),\ 0<t\le T, \tag{1.4}$$

Received: 10 November 2022; Accepted: 22 April 2024.
∗ Corresponding author. b-sepehrian@araku.ac.ir:

where $f(x,t)$, $g(x)$, $h_1(t)$ and $h_2(t)$ are known complex functions, $i^2=-1$, the parameters η and q are real constans. ${}^cD_t^\alpha$ denotes the Caputo fractional derivative of order $\alpha\in(0,1)$ defined by

$$ {}^cD_t^\alpha\ \psi(x,t)=\frac{1}{\Gamma(1-\alpha)}\int_0^t(t-\zeta)^{-\alpha}\ \frac{\partial\psi(x,\zeta)}{\partial\zeta}d\zeta. \tag{1.5}$$

Also, $\dfrac{\partial^\gamma}{\partial|x|^\gamma}$ is the Riesz derivative of order $\gamma\in(1,2)$ defined by

$$\frac{\partial^\gamma\psi(x,t)}{\partial|x|^\gamma}=-c_\gamma\Big[{}_aD_x^\gamma\psi(x,t)+{}_xD_b^\gamma\psi(x,t)\Big], \tag{1.6}$$

where $c_\gamma=\dfrac{1}{2\cos(\frac{\pi\gamma}{2})}$, and

$${}_aD_x^\gamma\psi(x,t)=\frac{1}{\Gamma(2-\gamma)}\frac{d^2}{dx^2}\int_a^x(x-\zeta)^{1-\gamma}\psi(\zeta,t)d\zeta, \tag{1.7}$$

$${}_xD_b^\gamma\psi(x,t)=\frac{1}{\Gamma(2-\gamma)}\frac{d^2}{dx^2}\int_x^b(\zeta-x)^{1-\gamma}\psi(\zeta,t)d\zeta. \tag{1.8}$$

are respectively the left and right-sided Riemann-Liouville fractional derivatives. These fractional derivatives are linear operators [24].

Lemma 1.1. For the Riemann-Liouville fractional derivatives we have [24]

$${}_aD_x^\gamma 1=\frac{1}{\Gamma(1-\gamma)}(x-a)^{-\gamma}, \tag{1.9}$$

$${}_xD_b^\gamma 1=\frac{1}{\Gamma(1-\gamma)}(b-x)^{-\gamma}. \tag{1.10}$$

Theorem 1.2. The Riemann-Liouville fractional derivatives of the power functions satisfy [24]

$${}_aD_x^\gamma\ (x-a)^p=\frac{\Gamma(p+1)}{\Gamma(p+1-\gamma)}(x-a)^{p-\gamma}, \tag{1.11}$$

$${}_xD_b^\gamma(b-x)^p=\frac{\Gamma(p+1)}{\Gamma(p+1-\gamma)}(b-x)^{p-\gamma}, \tag{1.12}$$

where $n-1<\gamma<n$, $p>-1$ and $p\in\mathbb{R}$.

There is not any method for obtaining the exact solution of the nonlinear TSFSE. Researchers have presented various numerical and approximating techniques for solving the nonlinear TSFSE. In [10] an adomian decomposition method, in [19] a finite difference scheme, and in [13] a finite element technique are proposed to investigate the nonlinear TSFSE. For further study see for example [1, 9, 11, 18, 31–33, 35].
There are only a few methods for solving the nonlinear time- and space-fractional PDEs. On the other hand, in most of the methods introduced for solving fractional PDEs, the finite difference and finite elements methods are applied for discretizing the fractional derivatives, while the fractional derivatives are non-local differential operators and so the radial basis functions (RBFs) method (as a non-local method) are more efficient for discretizing them. Moreover, the RBFs methods are usually more accurate than those methods, because the interpolating of smooth data using global, infinitely differentiable RBFs has a spectral accuracy [2, 4, 17, 20]. Also, unlike those methods, the RBFs methods are efficient for problems with irregular domain, because no mesh generation is needed in RBFs methods [23]. However, only a few RBFs methods have been presented to solve the fractional PDEs. Roughly speaking, no technique has yet been introduced to solve the time- and space-fractional PDEs by the RBFs. For these reasons, we were motivated to

propose a RBF method to solve TSFSE.
The RBFs may be applied to interpolate a function $f(\mathbf{x})$ at the distinct points $\mathbf{x}_1, \mathbf{x}_2, \ldots, \mathbf{x}_M$ as

$$f(\mathbf{x}) \approx \sum_{i=1}^{M} c_i \phi_i(\mathbf{x}), \quad \mathbf{x} \in \mathbb{R}^d, \tag{1.13}$$

in which $\phi_i(\mathbf{x}) = \phi(\|\mathbf{x} - \mathbf{x}_i\|_2)$ is radial basis function, c_i's are scalars to be determined in such a way that Eq. (5) is satisfied as equality for $\mathbf{x}_j$'s, and d is the dimension of problem. Thus a linear system of algebraic equations is obtained as

$$AC = b,$$

in which $C = (c_1, c_2, ..., c_M)^T$ is an unknown vector to be determined, $b = [f(\mathbf{x}_1), f(\mathbf{x}_2), ..., f(\mathbf{x}_M)]^T$ is the right-hand side vector, and the RBF interpolation matrix is given by

$$A = [\Phi_{ij}] = [\phi(\|\mathbf{x}_i - \mathbf{x}_j\|_2)]_{1 \le i,j \le M}.$$

The coefficients matrix, A, has usually a very large condition number i.e. A is very ill-conditioned. This is a major problem in RBF interpolation.
In this study, we use the Gaussian basis functions

$$\phi(r) = e^{-\varepsilon r^2}, \tag{1.14}$$

where, ε is called shape parameter that controls the flatness of the function. As the shape parameter becomes smaller, a better accuracy is obtained. But the smaller shape parameter causes the condition number of the interpolation matrix increase rapidly. To solve this issue, Fasshauer *et al.* proposed a stable method to compute and evaluate the Gaussian RBF interpolants [7]. Their method was based on Mercer's theorem and the eigenfunction expansion of the Gaussian RBF. They showed that the main sources of ill-conditioning are the eigenvalues of Gaussian RBF. So, to overcome the ill-conditioning, they introduced the mentioned stable method to write the interpolant independent of these eigenvalues. Moreover, they showed that the eigenfunctions of the Gaussian RBF can be written in terms of Hermite polynomials. Laterally, the authors in [26] showed that these eigenfunctions can be rewritten in terms of the shifted Chebyshev polynomials, and this can improve the stability of the Gaussian RBF interpolation. In fact, in the stable Gaussian RBF method, while using the capabilities of the RBFs, we do not encounter their main drawback, which is ill-conditioning.

The stable Gaussian RBF method has not yet been applied for the fractional problems, although some standard (non-fractional) ODEs and PDEs have been solved via it (e.g., see [26–28]). In this work, we apply the Gaussian RBF interpolant with the Chebyshev polynomials type eigenfunctions for TSFSE (1). Since the spatial derivative is of fractional type, for our development, we obtain the left- and right-sided Riemann-Liouville fractional derivatives of the eigenfunctions of the Gaussian RBF. Then, by a method of lines we reduce the problem to a coupled system of fractional ODEs. To solve the obtained system of ODEs, we present a high order finite difference method.

Next sections of the paper are as follows: Chebyshev polynomials and stable Gaussian RBF interpolation are described, in section 2. In section 3, the left- and right-sided Riemann-Liouville derivatives of the eigenfunction expansions based on Chebyshev polynomials are obtained. In section 4, we illustrate our method for solving Eq. (1) and then we extend the method for the two dimensional TSFSE. To certify the ability of the new method, several numerical illustrations are provided in section 5.

2. Preliminaries

2.1. **Chebyshev polynomials.** The Chebyshev polynomial of degree n for $n = 0$, $n = 1$ and $n \ge 2$, is as follows: $T_0(x) = 1$, $T_1(x) = x$ and

$$T_{n+1}(x) = 2xT_n(x) - T_{n-1}(x), \ n = 1, 2, \ldots$$

where $x \in [-1,1]$. For $n = 1, 2, \ldots$, $T_n(x)$, has $n+1$ extrema points as

$$x_j = \cos\frac{\pi(j-1)}{n}, \ j = 1, 2, \ldots, n+1.$$

2.2. **Stable Gaussian RBF interpolation.** The Gaussian RBF can be expanded in terms of eigenvalues $\lambda_n > 0$ and normalized eigenfunctions ϕ_n as [7, 26]

$$e^{-\varepsilon(x-z)^2} = \sum_{n=1}^{\infty} \lambda_n \phi_n(x)\phi_n(z), \tag{2.1}$$

in which the functions

$$\phi_n(x) = \sqrt{\beta} e^{-\delta^2 x^2} \tilde{H}_{n-1}(\sigma\beta x), \quad n = 1, 2, \cdots \tag{2.2}$$

are the orthogonal functions with respect to the weight function $w(x) = \frac{\sigma}{\sqrt{\pi}} e^{-\sigma^2 x^2}$, $\sigma > 0$. In (2.2), $\tilde{H}_n(x)$, $n = 0, 1, , \ldots$ is the normalized Hermite polynomial of degree n. Moreover,

$$\beta = \left(1 + \frac{4\varepsilon^2}{\sigma^2}\right)^{\frac{1}{4}}, \ \delta^2 = \frac{\sigma^2}{2}(\beta^2 - 1),$$

and

$$\lambda_n = \sqrt{\frac{\sigma^2}{\sigma^2 + \varepsilon^2 + \delta^2}} \left(\frac{\varepsilon^2}{\sigma^2 + \varepsilon^2 + \delta^2}\right)^{n-1}.$$

The Gaussian RBF interpolant of $f(x)$ at $x_1, x_2, \cdots, x_M$ is as

$$s_f(x) = \sum_{j=1}^{M} c_j e^{-\varepsilon(x-x_j)^2}, \tag{2.3}$$

where c_j's are scalars to be determined in such a way that the interpolation conditions $s_f(x_i) = f(x_i)$, $i = 1, \ldots, M$ are satisfied.
In practice, by choosing M terms of the series in (2.1), we approximate $e^{-\varepsilon(x-z)^2}$, and consequently we can rewrite (2.3) as

$$s_f(x) = \sum_{j=1}^{M} c_j \sum_{n=1}^{M} \lambda_n \phi_n(x)\phi_n(x_j). \tag{2.4}$$

Usually, the eigenvalues λ_n rapidly tend to zero as n increases, and this leads to ill-conditioning [22]. In [5, 26] the authors showed that $s_f(x)$ can be written independent of eigenvalues λ_j and coefficients c_j as

$$s_f(x) = W_\phi^T(x) \ \Phi_{\mathbf{X}}^{-T} \ \mathbf{f}, \tag{2.5}$$

where $W_\phi^T(x) = [\phi_1(x), ..., \phi_M(x)]$, $\mathbf{f} = [f(x_1), ..., f(x_M)]^T$, and

$$\Phi_{\mathbf{X}} = \begin{bmatrix} \phi_1(x_1) & \ldots & \phi_1(x_M) \\ \vdots & & \vdots \\ \phi_M(x_1) & \ldots & \phi_M(x_M) \end{bmatrix}. \tag{2.6}$$

The Hermite polynomials can grow dramatically and it can lead to instability in our computations. For this reason, in [28] the authors rebuilt the eigenfunctions as

$$\phi_n(x) = \sqrt{\beta} e^{-\delta^2 x^2} \hat{T}_{n-1}(x), \ n = 1, \ldots, M, \tag{2.7}$$

in which $\hat{T}_{n-1}$'s are the shifted Chebyshev polynomials on the interval $[0,1]$ that are given by

$$\hat{T}_n(x) = \begin{cases} \dfrac{1}{\sqrt{M}}, & n = 0, \\ \sqrt{\dfrac{2}{M}}\, T_n(2x-1), & n \geq 1. \end{cases}$$

The shifted Chebyshev polynomial of degree n can be presented by the analytical form [6]

$$\hat{T}_n(x) = \begin{cases} \dfrac{1}{\sqrt{M}}, & n = 0, \\ \sqrt{\dfrac{2}{M}}\, n \displaystyle\sum_{i=0}^{n} (-1)^{n-i} \frac{2^{2i}(n+i-1)!}{(2i)!(n-i)!} x^i, & n \geq 1. \end{cases} \tag{2.8}$$

In our development, we apply the Gaussian RBF interpolant (2.5) with the eigenfunctions (2.7).

3. Fractional derivatives of $\phi_n(x)$

Here, we present a method for computing the left and right-sided Riemann-Liouville derivatives of the eigenfunctions given in (2.7).

By Eqs. (2.7) and (2.8) we have

$$\phi_n(x) = \begin{cases} \dfrac{\beta}{\sqrt{M}} e^{-\delta^2 x^2}, & n = 1, \\ \sqrt{\dfrac{2\beta}{M}}\, (n-1) e^{-\delta^2 x^2} \displaystyle\sum_{i=0}^{n-1} (-1)^{n-i-1} \frac{2^{2i}(n+i-2)!}{(2i)!(n-i-1)!} x^i, & n \geq 2. \end{cases} \tag{3.1}$$

Now, we substitute the maclaurin series expansion of $e^{-\delta^2 x^2}$ in (3.1). So, the following equations are obtained

$$\phi_1(x) = \sqrt{\frac{\beta}{M}} \sum_{k=0}^{\infty} \frac{(-\delta^2)^k}{k!} x^{2k}, \tag{3.2}$$

and

$$\phi_n(x) = \sqrt{\frac{2\beta}{M}} \sum_{k=0}^{\infty} \frac{(-\delta^2)^k}{k!}\, (n-1) \sum_{i=0}^{n-1} (-1)^{n-1-i} \frac{2^{2i}(n+i-2)!}{(2i)!(n-1-i)!} x^{i+2k}, \ n = 2, 3, \cdots. \tag{3.3}$$

In order to obtain the left-sided Riemann-Liouville fractional derivative of $\phi_1(x)$, we substitute the Taylor series expansion of x^{2k} about the point $x = a$ in (3.2), and we write

$$\phi_1(x) = \sqrt{\frac{\beta}{M}} \sum_{k=0}^{\infty} \frac{(-\delta^2)^k}{k!} \sum_{j=0}^{2k} \binom{2k}{j} a^{2k-j}\, (x-a)^j. \tag{3.4}$$

Therefore

$${}_aD_x^{\gamma} \phi_1(x) = \sqrt{\frac{\beta}{M}} \sum_{k=0}^{\infty} \frac{(-\delta^2)^k}{k!} \sum_{j=0}^{2k} \binom{2k}{j} a^{2k-j}\, {}_aD_x^{\gamma} (x-a)^j, \tag{3.5}$$

and using Eqs. (1.9) and (1.11), we get

$${}_aD_x^{\gamma} \phi_1(x) = \sqrt{\frac{\beta}{M}} \sum_{k=0}^{\infty} \frac{(-\delta^2)^k}{k!} \sum_{j=0}^{2k} \binom{2k}{j} a^{2k-j}\, \frac{\Gamma(j+1)}{\Gamma(j+1-\gamma)} (x-a)^{j-\gamma}. \tag{3.6}$$

In similar way, using Eqs. (1.9), (1.11), and (3.3), ${}_aD_x^\gamma\phi_n(x)$ for $n \geq 2$ is obtained as

$$
\begin{aligned}
{}_aD_x^\gamma\phi_n(x) &= \sqrt{\frac{2\beta}{M}} \sum_{k=0}^{\infty} \frac{(-\delta^2)^k}{k!} \ (n-1) \sum_{i=0}^{n-1} (-1)^{n-i-1} \frac{2^{2i}(n+i-2)!}{(2i)!(n-i-1)!} \\
&\times \sum_{j=0}^{i+2k} \binom{i+2k}{j} a^{i+2k-j} \ \frac{\Gamma(j+1)}{\Gamma(j+1-\gamma)} (x-a)^{j-\gamma}.
\end{aligned} \tag{3.7}
$$

In order to calculate the right-sided Riemann-Liouville fractional derivative of $\phi_1(x)$, we substitute the Taylor series expansion of x^{2k} about the point $x = b$ in (3.2). Thus

$$
\phi_1(x) = \sqrt{\frac{\beta}{M}} \sum_{k=0}^{\infty} \frac{(-\delta^2)^k}{k!} \sum_{j=0}^{2k} \binom{2k}{j} b^{2k-j} (-1)^j \ (b-x)^j, \tag{3.8}
$$

and so using Eqs. (1.10) and (1.12) we obtain

$$
\begin{aligned}
{}_xD_b^\gamma\phi_1(x) &= \sqrt{\frac{\beta}{M}} \sum_{k=0}^{\infty} \frac{(-\delta^2)^k}{k!} \sum_{j=0}^{2k} \binom{2k}{j} b^{2k-j} (-1)^j \ {}_xD_b^\gamma (b-x)^j \\
&= \sqrt{\frac{\beta}{M}} \sum_{k=0}^{\infty} \frac{(-\delta^2)^k}{k!} \sum_{j=0}^{2k} \binom{2k}{j} b^{2k-j} (-1)^j \ \frac{\Gamma(j+1)}{\Gamma(j+1-\gamma)} (b-x)^{j-\gamma}.
\end{aligned} \tag{3.9}
$$

Similarly, by using Eqs. (1.10), (1.12), and (3.3), ${}_xD_b^\gamma\phi_n(x)$ for $n \geq 2$ is determined as

$$
\begin{aligned}
{}_xD_b^\gamma\phi_n(x) &= \sqrt{\frac{2\beta}{M}} \sum_{k=0}^{\infty} \frac{(-\delta^2)^k}{k!} \ (n-1) \sum_{i=0}^{n-1} (-1)^{n-i-1} \frac{2^{2i}(n+i-2)!}{(2i)!(n-i-1)!} \\
&\times \sum_{j=0}^{i+2k} \binom{i+2k}{j} b^{i+2k-j} (-1)^j \frac{\Gamma(j+1)}{\Gamma(j+1-\gamma)} (b-x)^{j-\gamma}.
\end{aligned} \tag{3.10}
$$

4. Solution of TSFSE

4.1. **One-Dimensional case.** First, we describe our method for one-dimensional TSFSE. For this purpose, we splite the unknown function $\psi(x,t)$ into its real and imaginary parts, as follows:

$$
\psi(x,t) = u(x,t) + iv(x,t), \tag{4.1}
$$

where

$$
|\psi(x,t)|^2 = u^2(x,t) + v^2(x,t). \tag{4.2}
$$

By replacing (1.6), (4.1) and (4.2) in (1.1), we get a coupled system as follows:

$$
\begin{aligned}
&{}^cD_t^\alpha u(x,t) - \eta \ c_\gamma \Big[{}_0D_x^\gamma v(x,t) + {}_xD_1^\gamma v(x,t) \Big] + q\Big(u^2(x,t) + v^2(x,t)\Big) v(x,t) = \text{Im } f(x,t), \\
&{}^cD_t^\alpha v(x,t) + \eta \ c_\gamma \Big[{}_0D_x^\gamma u(x,t) + {}_xD_1^\gamma u(x,t) \Big] - q\Big(u^2(x,t) + v^2(x,t)\Big) u(x,t) = -\text{Re } f(x,t).
\end{aligned} \tag{4.3}
$$

Also, substituting (4.1) in Eqs. (2)-(4) gives

$$
u(x,0) = \text{Re } g(x), \ v(x,0) = \text{Im } g(x), \ a \leq x \leq b, \tag{4.4}
$$

$$
u(a,t) = \text{Re } h_1(t), \ v(a,t) = \text{Im } h_1(t), \ 0 < t \leq T, \tag{4.5}
$$

$$
u(b,t) = \text{Re } h_2(t), \ v(b,t) = \text{Im } h_2(t), \ 0 < t \leq T. \tag{4.6}
$$

Now, we consider the distinct points $x_1, x_2, \ldots, x_M$ where $x_1 = a$ and $x_M = b$, and we discretize Eqs. (35) in the points $x_2, \ldots, x_{M-1}$ as

$$\begin{aligned} &{}^cD_t^\alpha u_i(t) - \eta\ c_\gamma \Big[{}_0D_x^\gamma v(x,t) + {}_xD_1^\gamma v(x,t) \Big]_{x=x_i} + q\Big(u_i^2(t) + v_i^2(t)\Big) v_i(t) = \text{Im } f(x_i,t), \\ &{}^cD_t^\alpha v_i(t) + \eta\ c_\gamma \Big[{}_0D_x^\gamma u(x,t) + {}_xD_1^\gamma u(x,t) \Big]_{x=x_i} - q\Big(u_i^2(t) + v_i^2(t)\Big) u_i(t) = -\text{Re } f(x_i,t), \end{aligned} \tag{4.7}$$

in which $u_i(t) = u(x_i,t)$ and $v_i(t) = v(x_i,t)$.
Using Eq. (2.5), we write

$$u(x,t) \approx W_\phi^T(x)\ \Phi_X^{-T}\ U(t), \tag{4.8}$$

$$v(x,t) \approx W_\phi^T(x)\ \Phi_X^{-T}\ V(t), \tag{4.9}$$

where $U(t) = \Big[u_1(t), u_2(t), \ldots, u_M(t)\Big]^T$ and $V(t) = \Big[v_1(t), v_2(t), \ldots, v_M(t)\Big]^T$, in which $u_1(t) = u(a,t)$, $u_M(t) = u(b,t)$, $v_1(t) = v(a,t)$ and $v_M(t) = v(b,t)$ are given by boundary conditions (37) and (38).
Substituting (4.8) and (4.9) in the coupled system (4.7) gives

$$\begin{aligned} &{}^cD_t^\alpha u_i(t) - \eta\ c_\gamma \Big[{}_0D_x^\gamma W_\phi^T(x_i)\ \Phi_X^{-T}\ V(t) + {}_xD_1^\gamma W_\phi^T(x_i)\ \Phi_X^{-T}\ V(t) \Big] + q\Big(u_i^2(t) + v_i^2(t)\Big) v_i(t) \\ &= \text{Im } f(x_i,t), \\ &{}^cD_t^\alpha v_i(t) + \eta\ c_\gamma \Big[{}_0D_x^\gamma W_\phi^T(x_i)\ \Phi_X^{-T}\ U(t) + {}_xD_1^\gamma W_\phi^T(x_i)\ \Phi_X^{-T}\ U(t) \Big] - q\Big(u_i^2(t) + v_i^2(t)\Big) u_i(t) \\ &= -\text{Re } f(x_i,t), \end{aligned} \tag{4.10}$$

where

$${}_0D_x^\gamma W_\phi^T(x_i) = \Big[{}_0D_x^\gamma \phi_1(x_i), ..., {}_0D_x^\gamma \phi_M(x_i) \Big],\ \ i = 2, \ldots, M-1,$$

and

$${}_xD_1^\gamma W_\phi^T(x_i) = \Big[{}_xD_1^\gamma \phi_1(x_i), ..., {}_xD_1^\gamma \phi_M(x_i) \Big],\ \ i = 2, \ldots, M-1,$$

are obtained by Eqs. (3.6), (3.7), (3.9) and (3.10).
Eqs. (4.10) give a coupled system of fractional ODEs in unknowns $u_2(t), \ldots, u_{M-1}(t)$ and $v_2(t), \ldots, v_{M-1}(t)$. We obtain the structure of this system as follows: We decompose $U(t)$ to two vectors $U_{\mathcal{B}}(t)$ and $U_{\mathcal{I}}(t)$ that are the boundrary and interior entries, respectively. Similarly, $V_{\mathcal{B}}(t)$ and $V_{\mathcal{I}}(t)$ are the boundrary and interior entries of $V(t)$. We set

$${}_0\tilde{\Psi}_X^T = \begin{bmatrix} {}_0D_x^\gamma W_\phi^T(x_2) \\ \vdots \\ {}_0D_x^\gamma W_\phi^T(x_{M-1}) \end{bmatrix},\ {}_1\tilde{\Psi}_X^T = \begin{bmatrix} {}_xD_1^\gamma W_\phi^T(x_2) \\ \vdots \\ {}_xD_1^\gamma W_\phi^T(x_{M-1}) \end{bmatrix},$$

$\bar{\bar{A}} = [\bar{\bar{a}}_{ij}] = {}_0\tilde{\Psi}_X^T\ \Phi_X^{-T}$ and $\bar{A} = [\bar{a}_{ij}] = {}_1\tilde{\Psi}_X^T\ \Phi_X^{-T}$. So, we have

$${}_0\tilde{\Psi}_X^T\ \Phi_X^{-T} U(t) = \underbrace{\begin{bmatrix} \bar{\bar{a}}_{1,1} & \bar{\bar{a}}_{1,M} \\ \bar{\bar{a}}_{2,1} & \bar{\bar{a}}_{2,M} \\ \vdots & \vdots \\ \bar{\bar{a}}_{M-2,1} & \bar{\bar{a}}_{M-2,M} \end{bmatrix}}_{=\bar{\bar{A}}_{\mathcal{B}}} \underbrace{\begin{bmatrix} u_1(t) \\ u_M(t) \end{bmatrix}}_{=U_{\mathcal{B}}(t)} + \underbrace{\begin{bmatrix} \bar{\bar{a}}_{1,2} & \ldots & \bar{\bar{a}}_{1,M-1} \\ \bar{\bar{a}}_{2,2} & \ldots & \bar{\bar{a}}_{2,M-1} \\ \vdots & \ldots & \vdots \\ \bar{\bar{a}}_{M-2,2} & \ldots & \bar{\bar{a}}_{M-2,M-1} \end{bmatrix}}_{=\bar{\bar{A}}_{\mathcal{I}}} \underbrace{\begin{bmatrix} u_2(t) \\ \vdots \\ u_{M-1}(t) \end{bmatrix}}_{=U_{\mathcal{I}}(t)},$$

and

$$ {}_1\tilde{\Psi}_X^T\ \Phi_X^{-T}U(t) = \underbrace{\begin{bmatrix} \bar{a}_{1,1} & \bar{a}_{1,M} \\ \bar{a}_{2,1} & \bar{a}_{2,M} \\ \vdots & \vdots \\ \bar{a}_{M-2,1} & \bar{a}_{M-2,M} \end{bmatrix}}_{=\bar{A}_{\mathcal{B}}} \underbrace{\begin{bmatrix} u_1(t) \\ u_M(t) \end{bmatrix}}_{=U_{\mathcal{B}}(t)} + \underbrace{\begin{bmatrix} \bar{a}_{1,2} & \dots & \bar{a}_{1,M-1} \\ \bar{a}_{2,2} & \dots & \bar{a}_{2,M-1} \\ \vdots & \dots & \vdots \\ \bar{a}_{M-2,2} & \dots & \bar{a}_{M-2,M-1} \end{bmatrix}}_{=\bar{A}_{\mathcal{I}}} \underbrace{\begin{bmatrix} u_2(t) \\ \vdots \\ u_{M-1}(t) \end{bmatrix}}_{=U_{\mathcal{I}}(t)}. $$

Similarly, ${}_0\tilde{\Psi}_X^T\ \Phi_X^{-T}V(t) = \bar{\bar{A}}_{\mathcal{I}}V_{\mathcal{I}}(t) + \bar{\bar{A}}_{\mathcal{B}}V_{\mathcal{B}}(t)$ and ${}_1\tilde{\Psi}_X^T\ \Phi_X^{-T}V(t) = \bar{A}_{\mathcal{I}}V_{\mathcal{I}}(t) + \bar{A}_{\mathcal{B}}V_{\mathcal{B}}(t)$ are gained and we can rewrite (4.10) as

$$ \begin{aligned} {}^cD_t^{\alpha}U_{\mathcal{I}}(t) - \eta\ c_{\gamma}\Big[(\bar{\bar{A}}_{\mathcal{I}} + \bar{A}_{\mathcal{I}})V_{\mathcal{I}}(t) + (\bar{\bar{A}}_{\mathcal{B}} + \bar{A}_{\mathcal{B}})V_{\mathcal{B}}(t)\Big] + q\ \mathcal{L}_V(t) &= F_1(t), \\ {}^cD_t^{\alpha}V_{\mathcal{I}}(t) + \eta\ c_{\gamma}\Big[(\bar{\bar{A}}_{\mathcal{I}} + \bar{A}_{\mathcal{I}})U_{\mathcal{I}}(t) + (\bar{\bar{A}}_{\mathcal{B}} + \bar{A}_{\mathcal{B}})U_{\mathcal{B}}(t)\Big] - q\ \mathcal{L}_U(t) &= -F_2(t), \end{aligned} \tag{4.11} $$

where

$$ \mathcal{L}_V(t) = \begin{bmatrix} \Big(U^2(x_2,t) + V^2(x_2,t)\Big)V(x_2,t) \\ \vdots \\ \Big(U^2(x_{M-1},t) + V^2(x_{M-1},t)\Big)V(x_{M-1},t) \end{bmatrix}, $$

$$ \mathcal{L}_U(t) = \begin{bmatrix} \Big(U^2(x_2,t) + V^2(x_2,t)\Big)U(x_2,t) \\ \vdots \\ \Big(U^2(x_{M-1},t) + V^2(x_{M-1},t)\Big)U(x_{M-1},t) \end{bmatrix}, $$

$$ F_1(t) = \begin{bmatrix} \text{Im } f(x_2,t) \\ \vdots \\ \text{Im } f(x_{M-1},t) \end{bmatrix}, $$

$$ F_2(t) = \begin{bmatrix} \text{Re } f(x_2,t) \\ \vdots \\ \text{Re } f(x_{M-1},t) \end{bmatrix}. $$

To solve the fractional system (4.11), we discretize its equations in the time direction as

$$ \begin{aligned} {}^cD_t^{\alpha}U_{\mathcal{I}}(t^n) - \eta\ c_{\gamma}\Big[(\bar{\bar{A}}_{\mathcal{I}} + \bar{A}_{\mathcal{I}})V_{\mathcal{I}}(t^n) + (\bar{\bar{A}}_{\mathcal{B}} + \bar{A}_{\mathcal{B}})V_{\mathcal{B}}(t^n)\Big] + q\ \mathcal{L}_V(t^n) &= F_1(t^n), \\ {}^cD_t^{\alpha}V_{\mathcal{I}}(t^n) + \eta\ c_{\gamma}\Big[(\bar{\bar{A}}_{\mathcal{I}} + \bar{A}_{\mathcal{I}})U_{\mathcal{I}}(t^n) + (\bar{\bar{A}}_{\mathcal{B}} + \bar{A}_{\mathcal{B}})U_{\mathcal{B}}(t^n)\Big] - q\ \mathcal{L}_U(t^n) &= -F_2(t^n), \end{aligned} \tag{4.12} $$

where $t^n = n\tau$ for $n = 0, 1, \ldots, N$ and τ is time step size. Now, we approximate ${}^cD_t^\alpha U_{\mathcal{I}}(t^n)$ and ${}^cD_t^\alpha V_{\mathcal{I}}(t^n)$ for $n = 1$, $n = 2$ and $n \geq 3$ by the method presented in [3] as

$$
\begin{aligned}
&{}^cD_t^\alpha U_{\mathcal{I}}(t^1) = \mu a_0\Big(U_{\mathcal{I}}(t^1) - U_{\mathcal{I}}(t^0)\Big) + O(\tau^{2-\alpha}), && (4.13)\\
&{}^cD_t^\alpha U_{\mathcal{I}}(t^2) = \mu\Big[(b_0 - a_1)U_{\mathcal{I}}(t^0) + (a_1 - a_0 - 2b_0)U_{\mathcal{I}}(t^1) + (a_0 + b_0)U_{\mathcal{I}}(t^2)\Big] + O(\tau^{3-\alpha}), && (4.14)\\
&{}^cD_t^\alpha U_{\mathcal{I}}(t^n) = \mu\Big[(b_{n-2} - a_{n-1})U_{\mathcal{I}}(t^0) + (a_{n-1} - a_{n-2} - 2b_{n-2})U_{\mathcal{I}}(t^1) + (a_{n-2} + b_{n-2})U_{\mathcal{I}}(t^2)\\
&+ \sum_{k=3}^{n-1}\Big(w_{1,n-k}U_{\mathcal{I}}(t^k) + w_{2,n-k}U_{\mathcal{I}}(t^{k-1}) + w_{3,n-k}U_{\mathcal{I}}(t^{k-2}) + w_{4,n-k}U_{\mathcal{I}}(t^{k-3})\Big)\\
&+ w_{1,0}U_{\mathcal{I}}(t^n) + w_{2,0}U_{\mathcal{I}}(t^{n-1}) + w_{3,0}U_{\mathcal{I}}(t^{n-2}) + w_{4,0}U_{\mathcal{I}}(t^{n-3})\Big] + O(\tau^{4-\alpha}), \quad n \geq 3 && (4.15)
\end{aligned}
$$

and

$$
\begin{aligned}
&{}^cD_t^\alpha V_{\mathcal{I}}(t^1) = \mu a_0\Big(V_{\mathcal{I}}(t^1) - V_{\mathcal{I}}(t^0)\Big) + O(\tau^{2-\alpha}), && (4.16)\\
&{}^cD_t^\alpha V_{\mathcal{I}}(t^2) = \mu\Big[(b_0 - a_1)V_{\mathcal{I}}(t^0) + (a_1 - a_0 - 2b_0)V_{\mathcal{I}}(t^1) + (a_0 + b_0)V_{\mathcal{I}}(t^2)\Big] + O(\tau^{3-\alpha}), && (4.17)\\
&{}^cD_t^\alpha V_{\mathcal{I}}(t^n) = \mu\Big[(b_{n-2} - a_{n-1})V_{\mathcal{I}}(t^0) + (a_{n-1} - a_{n-2} - 2b_{n-2})V_{\mathcal{I}}(t^1) + (a_{n-2} + b_{n-2})V_{\mathcal{I}}(t^2)\\
&+ \sum_{k=3}^{n-1}\Big(w_{1,n-k}V_{\mathcal{I}}(t^k) + w_{2,n-k}V_{\mathcal{I}}(t^{k-1}) + w_{3,n-k}V_{\mathcal{I}}(t^{k-2}) + w_{4,n-k}V_{\mathcal{I}}(t^{k-3})\Big)\\
&+ w_{1,0}V_{\mathcal{I}}(t^n) + w_{2,0}V_{\mathcal{I}}(t^{n-1}) + w_{3,0}V_{\mathcal{I}}(t^{n-2}) + w_{4,0}V_{\mathcal{I}}(t^{n-3})\Big] + O(\tau^{4-\alpha}), \quad n \geq 3, && (4.18)
\end{aligned}
$$

in which

$$
\begin{aligned}
\mu &= \frac{\tau^{-\alpha}}{\Gamma(2-\alpha)},\\
a_j &= (j+1)^{1-\alpha} - j^{1-\alpha},\\
b_j &= \frac{(j+1)^{2-\alpha} - j^{2-\alpha}}{2-\alpha} - \frac{(j+1)^{1-\alpha} + j^{1-\alpha}}{2},\\
w_{1,j} &= \frac{1}{6}\Big[2(j+1)^{1-\alpha} - 11j^{1-\alpha}\Big] + \frac{1}{2-\alpha}\Big[(j+1)^{2-\alpha} - 2j^{2-\alpha}\Big]\\
&\quad + \frac{1}{(2-\alpha)(3-\alpha)}\Big[(j+1)^{3-\alpha} - j^{3-\alpha}\Big],\\
w_{2,j} &= \frac{1}{2}\Big[(j+1)^{1-\alpha} + 6j^{1-\alpha}\Big] - \frac{1}{2-\alpha}\Big[2(j+1)^{2-\alpha} - 5j^{2-\alpha}\Big]\\
&\quad - \frac{3}{(2-\alpha)(3-\alpha)}\Big[(j+1)^{3-\alpha} - j^{3-\alpha}\Big],\\
w_{3,j} &= -\frac{1}{2}\Big[2(j+1)^{1-\alpha} + 3j^{1-\alpha}\Big] + \frac{1}{2-\alpha}\Big[(j+1)^{2-\alpha} - 4j^{2-\alpha}\Big]\\
&\quad + \frac{3}{(2-\alpha)(3-\alpha)}\Big[(j+1)^{3-\alpha} - j^{3-\alpha}\Big],
\end{aligned}
$$

and

$$w_{4,j} = \frac{1}{6}\Big[(j+1)^{1-\alpha} + 2j^{1-\alpha}\Big] + \frac{1}{2-\alpha}j^{2-\alpha} - \frac{1}{(2-\alpha)(3-\alpha)} \times \Big[(j+1)^{3-\alpha} - j^{3-\alpha}\Big].$$

By replacing (4.13) and (4.16) in (4.12), the following finite differences equations are achieved:

$$\begin{aligned} &\mu U_{\mathcal{I}}(t^1) - \eta\, c_\gamma(\bar{\bar{A}}_{\mathcal{I}} + \bar{A}_{\mathcal{I}})V_{\mathcal{I}}(t^1) + q\, \mathcal{L}_V(t^1) = \eta\, c_\gamma(\bar{\bar{A}}_{\mathcal{B}} + \bar{A}_{\mathcal{B}})V_{\mathcal{B}}(t^1) + F_1(t^1) + \mu U_{\mathcal{I}}(t^0),\\ &\mu V_{\mathcal{I}}(t^1) + \eta\, c_\gamma(\bar{\bar{A}}_{\mathcal{I}} + \bar{A}_{\mathcal{I}})U_{\mathcal{I}}(t^1) - q\, \mathcal{L}_U(t^1) = -\eta\, c_\gamma(\bar{\bar{A}}_{\mathcal{B}} + \bar{A}_{\mathcal{B}})U_{\mathcal{B}}(t^1) - F_2(t^1) + \mu V_{\mathcal{I}}(t^0), \end{aligned} \tag{4.19}$$

in which $U_{\mathcal{B}}(t^1)$ and $V_{\mathcal{B}}(t^1)$ are obtained by boundary conditions (4.5) and (4.6), and $U_{\mathcal{I}}(t^0)$ and $V_{\mathcal{I}}(t^0)$ are given by initial conditions (4.4). By solving the above nonlinear system, the unknowns $U_{\mathcal{I}}(t^1)$ and $V_{\mathcal{I}}(t^1)$ are obtained. Then, the vectors $U(t^1)$ and $V(t^1)$ are formed. Finally, by substituting $U(t^1)$ and $V(t^1)$ in Eqs. (4.8) and (4.9), the real and imaginary parts of the unknown function $\psi(x,t^1)$ are achieved.
Similarly, by substituting (4.14) and (4.17) in (4.12), we get

$$\begin{aligned} &\mu(a_0+b_0)U_{\mathcal{I}}(t^2) - \eta\, c_\gamma(\bar{\bar{A}}_{\mathcal{I}} + \bar{A}_{\mathcal{I}})V_{\mathcal{I}}(t^2) + q\, \mathcal{L}_V(t^2) = \eta\, c_\gamma(\bar{\bar{A}}_{\mathcal{B}} + \bar{A}_{\mathcal{B}})V_{\mathcal{B}}(t^2) + F_1(t^2)\\ &- \mu\Big[(b_0-a_1)U_{\mathcal{I}}(t^0) + (a_1-a_0-2b_0)U_{\mathcal{I}}(t^1)\Big],\\ &\mu(a_0+b_0)V_{\mathcal{I}}(t^2) + \eta\, c_\gamma(\bar{\bar{A}}_{\mathcal{I}} + \bar{A}_{\mathcal{I}})U_{\mathcal{I}}(t^2) - q\, \mathcal{L}_U(t^2) = -\eta\, c_\gamma(\bar{\bar{A}}_{\mathcal{B}} + \bar{A}_{\mathcal{B}})U_{\mathcal{B}}(t^2) - F_2(t^2)\\ &- \mu\Big[(b_0-a_1)V_{\mathcal{I}}(t^0) + (a_1-a_0-2b_0)V_{\mathcal{I}}(t^1)\Big], \end{aligned}$$

which is a nonlinear coupled system in unknown vectors $U_{\mathcal{I}}(t^2)$ and $V_{\mathcal{I}}(t^2)$, and by solving it, we can form $U(t^2)$ and $V(t^2)$, and then we can compute $u(x,t^2)$ and $v(x,t^2)$ by Eqs. (40) and (41).
Inductively, for $n \geq 3$ by Eqs. (4.12), (4.15), and (4.18), we get

$$\begin{aligned} &\mu\, w_{1,0}U_{\mathcal{I}}(t^n) - \eta\, c_\gamma(\bar{\bar{A}}_{\mathcal{I}} + \bar{A}_{\mathcal{I}})V_{\mathcal{I}}(t^n) + q\, \mathcal{L}_V(t^n) = \eta\, c_\gamma(\bar{\bar{A}}_{\mathcal{B}} + \bar{A}_{\mathcal{B}})V_{\mathcal{B}}(t^n) + F_1(t^n)\\ &- \mu\Bigg[(b_{n-2}-a_{n-1})U_{\mathcal{I}}(t^0) + (a_{n-1}-a_{n-2}-2b_{n-2})U_{\mathcal{I}}(t^1) + (a_{n-2}+b_{n-2})U_{\mathcal{I}}(t^2)\\ &\sum_{k=3}^{n-1}\Big(w_{1,n-k}U_{\mathcal{I}}(t^k) + w_{2,n-k}U_{\mathcal{I}}(t^{k-1}) + w_{3,n-k}U_{\mathcal{I}}(t^{k-2}) + w_{4,n-k}U_{\mathcal{I}}(t^{k-3})\Big)\\ &+ w_{2,0}U_{\mathcal{I}}(t^{n-1}) + w_{3,0}U_{\mathcal{I}}(t^{n-2}) + w_{4,0}U_{\mathcal{I}}(t^{n-3})\Bigg],\\ &\mu\, w_{1,0}V_{\mathcal{I}}(t^n) + \eta\, c_\gamma(\bar{\bar{A}}_{\mathcal{I}} + \bar{A}_{\mathcal{I}})U_{\mathcal{I}}(t^n) - q\, \mathcal{L}_U(t^n) = -\eta\, c_\gamma(\bar{\bar{A}}_{\mathcal{B}} + \bar{A}_{\mathcal{B}})U_{\mathcal{B}}(t^n) - F_2(t^n)\\ &- \mu\Bigg[(b_{n-2}-a_{n-1})V_{\mathcal{I}}(t^0) + (a_{n-1}-a_{n-2}-2b_{n-2})V_{\mathcal{I}}(t^1) + (a_{n-2}+b_{n-2})V_{\mathcal{I}}(t^2)\\ &+ \sum_{k=3}^{n-1}\Big(w_{1,n-k}V_{\mathcal{I}}(t^k) + w_{2,n-k}V_{\mathcal{I}}(t^{k-1}) + w_{3,n-k}V_{\mathcal{I}}(t^{k-2}) + w_{4,n-k}V_{\mathcal{I}}(t^{k-3})\Big)\\ &+ w_{2,0}V_{\mathcal{I}}(t^{n-1}) + w_{3,0}V_{\mathcal{I}}(t^{n-2}) + w_{4,0}V_{\mathcal{I}}(t^{n-3})\Bigg]. \end{aligned}$$

By solving the above system $U_{\mathcal{I}}(t^n)$ and $V_{\mathcal{I}}(t^n)$ are obtained and consequently $u(x,t^n)$ and $v(x,t^n)$ are computed.

4.2. **Two-Dimensional case.** Now, we generalize the presented method for solving the two-dimensional nonlinear TSFSE as

$$i\,{}^cD_t^\alpha\psi(x,y,t)+\eta\frac{\partial^\gamma\psi(x,y,t)}{\partial|x|^\gamma}+\eta\frac{\partial^\gamma\psi(x,y,t)}{\partial|y|^\gamma}+q|\psi(x,y,t)|^2\psi(x,y,t)=f(x,y,t), \tag{4.20}$$

with the initial and boundary conditions

$$\begin{aligned}&\psi(x,y,0)=g(x,y),\\&\psi(0,y,t)=h_1(y,t),\\&\psi(1,y,t)=h_2(y,t),\\&\psi(x,0,t)=h_3(x,t),\\&\psi(x,1,t)=h_4(x,t).\end{aligned}$$

Similar to the one-dimensional case, we splite the unknown function into real and imaginary parts as follows:

$$\psi(x,y,t)=u(x,y,t)+iv(x,y,t), \tag{4.21}$$

where

$$|\psi(x,y,t)|^2=u^2(x,y,t)+v^2(x,y,t). \tag{4.22}$$

By replacing (6), (4.21) and (4.22) in Eq. (4.20), we get the below coupled system

$$\begin{aligned}&{}^cD_t^\alpha u(x,y,t)-\eta\ c_\gamma\Big[{}_0D_x^\gamma v(x,y,t)+{}_xD_1^\gamma v(x,y,t)+{}_0D_y^\gamma v(x,y,t)+{}_yD_1^\gamma v(x,y,t)\Big]\\&+q\Big(u^2(x,y,t)+v^2(x,y,t)\Big)v(x,y,t)=\text{Im }f(x,y,t),\\&{}^cD_t^\alpha v(x,y,t)+\eta\ c_\gamma\Big[{}_0D_x^\gamma u(x,y,t)+{}_xD_1^\gamma u(x,y,t)+{}_0D_y^\gamma u(x,y,t)+{}_yD_1^\gamma u(x,y,t)\Big]\\&-q\Big(u^2(x,y,t)+v^2(,yx,t)\Big)u(x,y,t)=-\text{Re }f(x,y,t).\end{aligned} \tag{4.23}$$

Also, substituting (4.21) in initial and boundary conditions gives

$$u(x,y,0)=\text{Re }g(x,y),\ v(x,y,0)=\text{Im }g(x,y),\ 0\le x,y\le 1, \tag{4.24}$$
$$u(0,y,t)=\text{Re }h_1(y,t),\ v(0,y,t)=\text{Im }h_1(y,t),\ 0<t\le T, \tag{4.25}$$
$$u(1,y,t)=\text{Re }h_2(y,t),\ v(1,y,t)=\text{Im }h_2(y,t),\ 0<t\le T, \tag{4.26}$$
$$u(x,0,t)=\text{Re }h_3(x,t),\ v(x,0,t)=\text{Im }h_3(x,t),\ 0<t\le T, \tag{4.27}$$
$$u(x,1,t)=\text{Re }h_4(x,t),\ v(x,1,t)=\text{Im }h_4(x,t),\ 0<t\le T. \tag{4.28}$$

We discretize Eqs. (4.23) in the spatial directions at the distinct points (x_i,y_j), $i=1,...,M_1$ and $j=1,...,M_2$ where (x_1,y_j), (x_{M_1},y_j), (x_i,y_1) and (x_i,y_{M_2}) are boundary points. Then, we approximate the real and imaginary parts by

$$u(x,y,t)=W_\phi^T(x)\ \Phi_X^{-T}\ U(t)\Phi_Y^{-1}W_\phi(y), \tag{4.29}$$
$$v(x,y,t)=V_\phi^T(x)\ \Phi_X^{-T}\ V(t)\Phi_Y^{-1}W_\phi(y), \tag{4.30}$$

in which $W_\phi(y)$ and Φ_Y are defined like $W_\phi(x)$ and Φ_X, respectively, and $U(t)=[u_{i,j}(t)]$ and $V(t)=[v_{i,j}(t)]$, where $u_{i,j}(t)=u(x_i,y_j,t)$ and $v_{i,j}(t)=v(x_i,y_j,t)$, for $i=1,..,M_1$, $j=1,...,M_2$.

Substituting (4.29), (4.30) in the discretized form of (4.23), we have

$$
\begin{aligned}
&{}^{c}D_t^{\alpha}u_{i,j}(t)-\eta\ c_\gamma\Big[{}_0D_x^{\gamma}W_\phi^T(x_i)\ \Phi_X^{-T}\ V(t)\Phi_Y^{-1}W_\phi(y_j)+{}_xD_1^{\gamma}W_\phi^T(x_i)\ \Phi_X^{-T}\ V(t)\Phi_Y^{-1}W_\phi(y_j)+\\
&W_\phi^T(x_i)\ \Phi_X^{-T}\ V(t)\Phi_Y^{-1}{}_0D_y^{\gamma}W_\phi(y_j)+W_\phi^T(x_i)\ \Phi_X^{-T}\ V(t)\Phi_Y^{-1}{}_yD_1^{\gamma}W_\phi(y_j)\Big]+q\Big(u_{i,j}^2t)+v_{i,j}^2(t)\Big)v_{i,j}(t)\\
&=\text{Im}\ f(x_i,y_j,t),
\end{aligned}
\tag{4.31}
$$

$$
\begin{aligned}
&{}^{c}D_t^{\alpha}v_{i,j}(t)+\eta\ c_\gamma\Big[{}_0D_x^{\gamma}W_\phi^T(x_i)\ \Phi_X^{-T}\ U(t)\Phi_Y^{-1}W_\phi(y_j)+{}_xD_1^{\gamma}W_\phi^T(x_i)\ \Phi_X^{-T}\ U(t)\Phi_Y^{-1}W_\phi(y_j)+\\
&W_\phi^T(x_i)\ \Phi_X^{-T}\ U(t)\Phi_Y^{-1}{}_0D_y^{\gamma}W_\phi(y_j)+W_\phi^T(x_i)\ \Phi_X^{-T}\ U(t)\Phi_Y^{-1}{}_yD_1^{\gamma}W_\phi(y_j)\Big]-q\Big(u_{i,j}^2(t)+v_{i,j}^2(t)\Big)u_{i,j}(t)\\
&=-\text{Re}\ f(x_i,y_j,t),
\end{aligned}
\tag{4.32}
$$

where ${}_0D_x^{\gamma}W_\phi^T(x_i)$, ${}_xD_1^{\gamma}W_\phi(x_i)$, ${}_0D_y^{\gamma}W_\phi^T(y_j)$ and ${}_yD_1^{\gamma}W_\phi(y_j)$ are obtained by Eqs. (28), (29), (31) and (32).
We generalize the structure presented in one-dimensional case to two-dimensional as follows:
We defined $\bar{\bar{B}}=[\bar{\bar{b}}_{ij}]=\Phi_Y^{-1}\ {}_0\tilde{\Psi}_Y$ and $\bar{B}=[\bar{b}_{ij}]=\Phi_Y^{-1}\ {}_1\tilde{\Psi}_Y$ where

$$
\begin{aligned}
&{}_0\tilde{\Psi}_Y=[{}_0D_y^{\gamma}W_\phi(y_2),\ldots,{}_0D_y^{\gamma}W_\phi(y_{M_2-1})],\\
&{}_1\tilde{\Psi}_Y=[{}_yD_1^{\gamma}W_\phi(y_2),\ldots,{}_yD_1^{\gamma}W_\phi(y_{M_2-1})].
\end{aligned}
$$

Also, we put

$$
\tilde{\Phi}_Y=[W_\phi(y_2),\ldots,W_\phi(y_{M_2-1})],\ \tilde{\Phi}_X^T=\begin{bmatrix}W_\phi^T(x_2)\\ \vdots\\ W_\phi^T(x_{M_1-1})\end{bmatrix}.
$$

The below relations are obtained easily

$$
\begin{aligned}
{}_0\tilde{\Psi}_X^T\ \Phi_X^{-T}V(t)\ \Phi_Y^{-1}\tilde{\Phi}_Y &= \underbrace{\begin{bmatrix} \bar{\bar{a}}_{1,1} & \bar{\bar{a}}_{1,M_2} \\ \bar{\bar{a}}_{2,1} & \bar{\bar{a}}_{2,M_2} \\ \vdots & \vdots \\ \bar{\bar{a}}_{M_1-2,1} & \bar{\bar{a}}_{M_1-2,M_2} \end{bmatrix}}_{=\bar{\bar{A}}_{\mathcal{B}}} \underbrace{\begin{bmatrix} v_{1,2}(t) & v_{1,3}(t) & \dots & v_{1,M_2-1}(t) \\ v_{M_1,2}(t) & v_{M_1,3}(t) & \dots & v_{M_1,M_2-1}(t) \end{bmatrix}}_{=V_{\mathcal{B}}^{row}(t)} \\
&+ \underbrace{\begin{bmatrix} \bar{\bar{a}}_{1,2} & \dots & \bar{\bar{a}}_{1,M_2-1} \\ \bar{\bar{a}}_{2,2} & \dots & \bar{\bar{a}}_{2,M_2-1} \\ \vdots & \dots & \vdots \\ \bar{\bar{a}}_{M_1-2,2} & \dots & \bar{\bar{a}}_{M_1-2,M_2-1} \end{bmatrix}}_{=\bar{\bar{A}}_{\mathcal{I}}} \\
&\times \underbrace{\begin{bmatrix} v_{2,2}(t) & v_{2,3}(t) & \dots & v_{2,M_2-1}(t) \\ v_{M_1-1,2}(t) & v_{M_1-1,3}(t) & \dots & v_{M_1-1,M_2-1}(t) \end{bmatrix}}_{=V_{\mathcal{I}}(t)}, \\
\tilde{\Phi}_X^T\ \Phi_X^{-T}V(t)\Phi_Y^{-1}{}_0\tilde{\Psi}_Y &= \underbrace{\begin{bmatrix} v_{2,1}(t) & v_{2,M_2}(t) \\ v_{3,1}(t) & v_{3,M_2}(t) \\ \vdots & \vdots \\ v_{M_1-1,1}(t) & v_{M_1-1,M_2}(t) \end{bmatrix}}_{=V_{\mathcal{B}}^{col}(t)} \underbrace{\begin{bmatrix} \bar{\bar{b}}_{1,1} & \bar{\bar{b}}_{1,2} & \dots & \bar{\bar{b}}_{1,M_2-2} \\ \bar{\bar{b}}_{M_1,1} & \bar{\bar{b}}_{M_1,2} & \dots & \bar{\bar{b}}_{M_1,M_2-2} \end{bmatrix}}_{=\bar{\bar{B}}_{\mathcal{B}}} \\
&+ \underbrace{\begin{bmatrix} v_{2,2}(t) & v_{2,3}(t) & \dots & v_{2,M_2-1}(t) \\ \vdots & \dots & \vdots & \\ v_{M_1-1,2}(t) & v_{M_1-1,3}(t) & \dots & v_{M_1-1,M_2-1}(t) \end{bmatrix}}_{=V_{\mathcal{I}}(t)} \\
&\times \underbrace{\begin{bmatrix} \bar{\bar{b}}_{2,1} & \bar{\bar{b}}_{2,2} & \dots & \bar{\bar{b}}_{2,M_2-2} \\ \vdots & \dots & \vdots & \\ \bar{\bar{b}}_{M_1-1,1} & \bar{\bar{b}}_{M_1-1,2} & \dots & \bar{\bar{b}}_{M_1-1,M_2-2} \end{bmatrix}}_{=\bar{\bar{B}}_{\mathcal{I}}}.
\end{aligned}
$$

Similarly, we have

$$
\begin{aligned}
{}_1\tilde{\Psi}_X^T\ \Phi_X^{-T}V(t)\ \Phi_Y^{-1}\tilde{\Phi}_Y &= \bar{A}_{\mathcal{I}}V_{\mathcal{I}}(t) + \bar{A}_{\mathcal{B}}V_{\mathcal{B}}^{row}(t), \\
{}_0\tilde{\Psi}_X^T\ \Phi_X^{-T}U(t)\ \Phi_Y^{-1}\tilde{\Phi}_Y &= \bar{\bar{A}}_{\mathcal{I}}U_{\mathcal{I}}(t) + \bar{\bar{A}}_{\mathcal{B}}U_{\mathcal{B}}^{row}(t), \\
{}_1\tilde{\Psi}_X^T\ \Phi_X^{-T}U(t)\ \Phi_Y^{-1}\tilde{\Phi}_Y &= \bar{A}_{\mathcal{I}}U_{\mathcal{I}}(t) + \bar{A}_{\mathcal{B}}U_{\mathcal{B}}^{row}(t), \\
\tilde{\Phi}_X^T\ \Phi_X^{-T}V(t)\Phi_Y^{-1}{}_1\tilde{\Psi}_Y &= V_{\mathcal{I}}(t)\bar{B}_{\mathcal{I}} + V_{\mathcal{B}}^{col}(t)\bar{B}_{\mathcal{B}}, \\
\tilde{\Phi}_X^T\ \Phi_X^{-T}U(t)\Phi_Y^{-1}{}_0\tilde{\Psi}_Y &= U_{\mathcal{I}}(t)\bar{\bar{B}}_{\mathcal{I}} + U_{\mathcal{B}}^{col}(t)\bar{\bar{B}}_{\mathcal{B}}, \\
\tilde{\Phi}_X^T\ \Phi_X^{-T}U(t)\Phi_Y^{-1}{}_1\tilde{\Psi}_Y &= U_{\mathcal{I}}(t)\bar{B}_{\mathcal{I}} + U_{\mathcal{B}}^{col}(t)\bar{B}_{\mathcal{B}}.
\end{aligned}
$$

Substituting the above equations in (4.31) and (4.32) gives a fractional system in the unknown matrices $U_{\mathcal{I}}$ and $V_{\mathcal{I}}$. The finite difference scheme proposed for one dimensional case can be easily developed for this fractional system.

5. Numerical illustrations

In this section, we apply the mentioned method to solve four numerical illustrations. We put a positive integer "$\mathcal{N}$" instead of "∞" in Eqs. (3.2)- (3.10). In all examples, $\mathcal{N} = 15$ is considered. Also, we utilize the Chebyshev extrema points on interval $[0, 1]$ as discretization points that are defined as:

$$x_j = -\frac{1}{2}\cos\frac{\pi(j-1)}{M-1} + \frac{1}{2},\ j = 1, 2, \ldots, M.$$

The numerical examples are implemented in **Maple 16** and **SageMath 8.8** software on a PC with an Intel(R) Core(TM) i5-4210U CPU, a 64-bit Windows 8.1 operating system, and 6 GB internal memory. The errors are computed at $t = t^N$ by the formulas

$$E_\infty = \Big\|u_{exact}(x, t^N) - u_{approx}(x, t^N)\Big\|_\infty = \max_{1\le i\le \mathcal{M}}\Big|u_{exact}(x_i, t^N) - u_{approx}(x_i, t^N)\Big|,$$

$$E_2 = \left[\sum_{i=1}^{\mathcal{M}}\Big(u_{exact}(x_i, t^N) - u_{approx}(x_i, t^N)\Big)^2\right]^{\frac{1}{2}},$$

$$RMSE = \left[\frac{1}{\mathcal{M}}\sum_{i=1}^{\mathcal{M}}\Big(u_{exact}(x_i, t^N) - u_{approx}(x_i, t^N)\Big)^2\right]^{\frac{1}{2}}.$$

The errors are computed with $\mathcal{M} = 101$ uniform points and $h = 0.01$, where $h = x_{i+1} - x_i$, $i = 1, \cdots, M-1$. Also, the following formula is used to compute the experimental convergence order $(C - Order)$ of the new method

$$C - Order = log_2\left(\frac{\ell(h, 2\tau)}{\ell(h, \tau)}\right),$$

where ℓ can be E_∞, E_2 and $RMSE$ errors. Moreover, the resulted nonlinear systems are solved by the Newton iterative method with the stop condition

$$\frac{\|X_{k+1} - X_k\|_\infty}{\|X_{k+1}\|_\infty} < 10^{-5}.$$

To start the Newton iteration method, for the first time step, we use the radial basis interpolation function $u(x, 0)$ and $v(x, 0)$, and then, for $n+1$th time step, the nth time step information is used.

Example 5.1. We solve the nonlinear TSFSE: [19]

$$i\,{}^cD_t^\alpha\psi(x,t) + \frac{\partial^\gamma\psi(x,t)}{\partial|x|^\gamma} + 2|\psi(x,t)|^2\psi(x,t) = f(x,t),$$

with

$$\psi(x, 0) = 0,\ 0 \le x \le 1,$$
$$\psi(0, t) = 0,\ 0 < t \le 1,$$
$$\psi(1, t) = 0,\ 0 < t \le 1,$$

where

$$f(x,t) = i\frac{\Gamma(4)}{\Gamma(4-\alpha)}t^{3-\alpha}x^2(1-x)^2 + 2t^9x^6(1-x)^6 - \frac{1}{\Gamma(5-\gamma)}t^3x^{-\gamma}$$
$$\times\left(\left(\frac{1}{1-x}\right)^\gamma(1-x)^2x^\gamma\Big(12x^2 - 6x\gamma + (-1+\gamma)\gamma\Big) + x^2\Big(12(1-x)^2\right.$$
$$\left.+ (-7+6x)\gamma + \gamma^2\Big)\right)\sec\left(\frac{\pi\gamma}{2}\right),$$

and $\psi(x,t) = t^3x^2(1-x)^2$ is the exact solution.
This problem has been investigated in [19] via a finite difference scheme. In Table 1, we compare the RMSE errors and $C-orders$ obtained by the present technique and method in [19] with the spatial step size $h = 0.00125$. Table 2 demonstrates our results for $M = 8, 9, 10, 11, 12$. Table 3 depicts the errors obtained by $M = 10$ and $\tau = 0.01$. As the table shows, the errors are very small even for $t = 3$ (300 iterations). So, we can conclude the method has a good stability for this problem.

TABLE 1. The RMSE errors and $C-orders$ for real part resulted by our method ($\varepsilon = 0.15$, $\sigma = 3$ and with $M = 10$), and method in [19], at $t = 1$ in Example 1 for $\alpha = 0.2$.

		Our method		Method in [19]	
γ	τ	RMSE	$C-order$	RMSE	$C-order$
1.3					
	$\frac{1}{8}$	5.99740×10^{-8}	–	1.0967×10^{-4}	–
	$\frac{1}{16}$	5.12219×10^{-9}	3.55	3.5127×10^{-5}	1.64
	$\frac{1}{32}$	4.17589×10^{-10}	3.62	1.0971×10^{-5}	1.67
	$\frac{1}{64}$	3.38902×10^{-11}	3.62	3.3709×10^{-6}	1.70
1.5					
	$\frac{1}{8}$	3.99647×10^{-8}	–	8.4755×10^{-5}	–
	$\frac{1}{16}$	3.27360×10^{-9}	3.61	2.7140×10^{-5}	1.64
	$\frac{1}{32}$	2.63262×10^{-10}	3.64	8.4748×10^{-6}	1.67
	$\frac{1}{64}$	2.17271×10^{-11}	3.60	2.6056×10^{-6}	1.70
1.7					
	$\frac{1}{8}$	2.40138×10^{-8}	–	6.3801×10^{-5}	–
	$\frac{1}{16}$	1.92259×10^{-9}	3.64	2.0426×10^{-5}	1.64
	$\frac{1}{32}$	1.53749×10^{-10}	3.64	6.3782×10^{-6}	1.67
	$\frac{1}{64}$	1.35151×10^{-11}	3.51	1.9644×10^{-6}	1.69
1.9					
	$\frac{1}{8}$	1.34096×10^{-8}	–	4.6971×10^{-5}	–
	$\frac{1}{16}$	1.06322×10^{-9}	3.66	1.5037×10^{-5}	1.64
	$\frac{1}{32}$	8.51438×10^{-11}	3.64	4.6976×10^{-6}	1.67
	$\frac{1}{64}$	8.80514×10^{-12}	3.27	1.4572×10^{-6}	1.68

TABLE 2. The comparison of E_∞ and E_2 errors and condition number of matrix ϕ_X for different values of M using presented method with $\alpha = 0.2$, $\gamma = 1.7$, $\varepsilon = 0.15$, $\sigma = 3$, $\tau = 0.015625$ at $t = 1$ in Example 1.

	Real part		Imaginary part		
M	E_∞	E_2	E_∞	E_2	$\kappa_\infty(\phi_X)$
8	2.04778×10^{-8}	1.10415×10^{-7}	5.66021×10^{-10}	3.93624×10^{-9}	8.3504
9	1.22321×10^{-10}	6.06866×10^{-10}	5.33926×10^{-11}	3.77159×10^{-10}	9.3609
10	2.32768×10^{-11}	1.35798×10^{-10}	5.29700×10^{-11}	3.75215×10^{-10}	10.372
11	1.68127×10^{-11}	1.21011×10^{-10}	5.28873×10^{-11}	3.74237×10^{-10}	11.384
12	1.68418×10^{-11}	1.21134×10^{-10}	5.29427×10^{-11}	3.74418×10^{-10}	12.396

TABLE 3. The comparison of E_2 and $RMSE$ errors for various values of t with $\alpha = 0.2$, $\gamma = 1.3$, $M = 10$ and $\varepsilon = 0.15$, $\sigma = 3$ at $\tau = 0.01$ in Example 1.

	Real part		Imaginary part	
t	E_2	$RMSE$	E_2	$RMSE$
0.5	1.268806×10^{-10}	1.262509×10^{-11}	3.279055×10^{-10}	3.262782×10^{-11}
1	8.360364×10^{-11}	8.318873×10^{-12}	1.396291×10^{-10}	1.389362×10^{-11}
1.5	1.739737×10^{-10}	1.731103×10^{-11}	9.117031×10^{-11}	9.071785×10^{-12}
2	3.967341×10^{-10}	3.947652×10^{-11}	8.705242×10^{-11}	8.662039×10^{-12}
2.5	7.920351×10^{-10}	7.881044×10^{-11}	2.431625×10^{-10}	2.419558×10^{-11}
3	6.191609×10^{-9}	6.160881×10^{-10}	4.070811×10^{-6}	4.050609×10^{-7}

Example 5.2. Consider [13]

$$i\,{}^{c}D_{t}^{\alpha}\psi(x,t) + \frac{\partial^{\gamma}\psi(x,t)}{\partial|x|^{\gamma}} + |\psi(x,t)|^{2}\psi(x,t) = f(x,t),$$

with

$$\begin{aligned}
&\psi(x,0) = 10x^{2}(1-x)^{2}, \ 0 \le x \le 1,\\
&\psi(0,t) = 0, \qquad 0 < t \le 0.5,\\
&\psi(1,t) = 0, \qquad 0 < t \le 0.5,
\end{aligned}$$

where

$$\begin{aligned}
f(x,t) = {} & i\frac{20t^{2-\alpha}}{\Gamma(3-\alpha)}x^{2}(1-x)^{2} + 1.0\times 10^{3}.(1+t^{2})^{3}x^{6}(1-x)^{6}\\
& - \frac{10(1+t^{2})x^{2-\gamma}}{\cos(\frac{\gamma\pi}{2})\Gamma(3-\gamma)} \times \left(1 - \frac{6x}{3-\gamma} + -\frac{12x^{2}}{(3-\gamma)(4-\gamma)}\right)\\
& - \frac{10(1+t^{2})(1-x)^{2-\gamma}}{\cos(\frac{\gamma\pi}{2})\Gamma(3-\gamma)} \times \left(1 - \frac{6(1-x)}{3-\gamma} + -\frac{12(1-x)^{2}}{(3-\gamma)(4-\gamma)}\right).
\end{aligned}$$

The function, $\psi(x,t) = 10(1+t^{2})x^{2}(1-x)^{2}$, is the exact solution.
This problem has been solved in [13] by a fully discrete finite elements method. We solve it by our technique. In Table 4, our results are compared with those presented in [13]. In Table 4, τ and h denote the temporal and spatial step sizes, respectively. Table 4 shows that as the temporal step size (τ) decreases, the errors become smaller. Table 5 depicts the errors and $\kappa_{\infty}(\phi_X)$ for different values of M, and confirms the convergence of our method and the well-conditioning of the interpolation matrix.

TABLE 4. The comparison of both E_∞ errors and $C-orders$ between presented method ($\varepsilon = 0.15$, $\sigma = 3$ and $M = 10$) and method in [13] with $h = 10^{-3}$, for $\alpha = 0.3$ and $\gamma = 1.2$, at $t = 0.5$ in Example 2.

	Real part		Imaginary part	
τ	E_2	$C-order$	E_2	$C-order$
Our method				
$\frac{1}{8}$	7.876322×10^{-5}	–	4.054167×10^{-4}	–
$\frac{1}{16}$	3.323861×10^{-5}	1.24	7.305892×10^{-5}	2.47
$\frac{1}{32}$	5.906817×10^{-6}	2.49	1.012731×10^{-5}	2.85
$\frac{1}{64}$	1.001845×10^{-6}	2.56	1.431507×10^{-6}	2.82
$\frac{1}{128}$	1.659518×10^{-7}	2.59	2.066758×10^{-7}	2.79
Method in [13]				
$\frac{1}{8}$	5.088096×10^{-4}	–	8.277816×10^{-4}	–
$\frac{1}{16}$	1.634896×10^{-4}	1.637928	2.747536×10^{-4}	1.591112
$\frac{1}{32}$	5.253915×10^{-5}	1.637734	8.933547×10^{-5}	1.620833
$\frac{1}{64}$	1.700971×10^{-5}	1.627034	2.858752×10^{-5}	1.643848
$\frac{1}{128}$	5.726426×10^{-6}	1.570652	8.980920×10^{-6}	1.670450

TABLE 5. The comparison of E_∞ and E_2 errors and condition number of matrix ϕ_X for different values of M using presented method with $\alpha = 0.3$, $\gamma = 1.6$, $\varepsilon = 0.2$, $\sigma = 3$, $\tau = 0.02$ at $t = 1$ in Example 2.

	Real part		Imaginary part		
M	E_∞	E_2	E_∞	E_2	$\kappa_\infty(\phi_X)$
8	1.53642×10^{-6}	7.47919×10^{-6}	1.55855×10^{-7}	1.09288×10^{-6}	8.4400
9	7.74849×10^{-8}	4.81321×10^{-7}	6.32069×10^{-8}	4.45266×10^{-7}	9.4616
10	6.73296×10^{-8}	4.74453×10^{-7}	6.29985×10^{-8}	4.44968×10^{-7}	10.484

Example 5.3. Consider the following nonlinear TSFSE:

$$i\,{}^cD_t^\alpha \psi(x,t) + \frac{\partial^\gamma \psi(x,t)}{\partial |x|^\gamma} + 2|\psi(x,t)|^2 \psi(x,t) = f(x,t),$$

with the non-smooth initial condition

$$\psi(x,0) = \begin{cases} x, & x < \frac{1}{2}, \\ 1-x, & x \geq \frac{1}{2}, \end{cases}, \quad 0 \leq x \leq 1,$$

and boundary conditions

$$\psi(0,t) = 0, \ 0 < t \leq 1,$$
$$\psi(1,t) = 0, \ 0 < t \leq 1,$$

where

$$f(x,t) = x^2 t^3 (xt + i).$$

In Table 6, we report the numerical approximations for different values of τ using the presented method. This table confirms the efficiency of the new technique even for a nonlinear TSFSE with non-smooth initial data. Figure 1 depicts the real and the imaginary parts of the approximate solution for $M = 12$ at the time $t = 1.5$.

TABLE 6. The numerical estimates using presented method with $\gamma = 1.7$, $\alpha = 0.15$, $M = 10$, $\varepsilon = 0.15$ and $\sigma = 3$ at $t = 1$ in Example 3.

(x,t)	$\tau = 0.02$	$\tau = 0.01$	$\tau = 0.005$	$\tau = 0.0025$
$u(0.2,1)$	-0.00387576	-0.00388277	-0.00388627	-0.00388802
$u(0.4,1)$	-0.01105906	-0.01106992	-0.01107534	-0.01107806
$u(0.6,1)$	-0.02188627	-0.02189714	-0.02190256	-0.02190527
$u(0.8,1)$	-0.02784189	-0.02784890	-0.02785239	-0.02785414
$v(0.2,1)$	-0.06431573	-0.06429290	-0.06428156	-0.06427591
$v(0.4,1)$	-0.10950439	-0.10946771	-0.10944950	-0.10944043
$v(0.6,1)$	-0.12454102	-0.12450432	-0.12448609	-0.12447701
$v(0.8,1)$	-0.09585389	-0.09583102	-0.09581966	-0.09581401

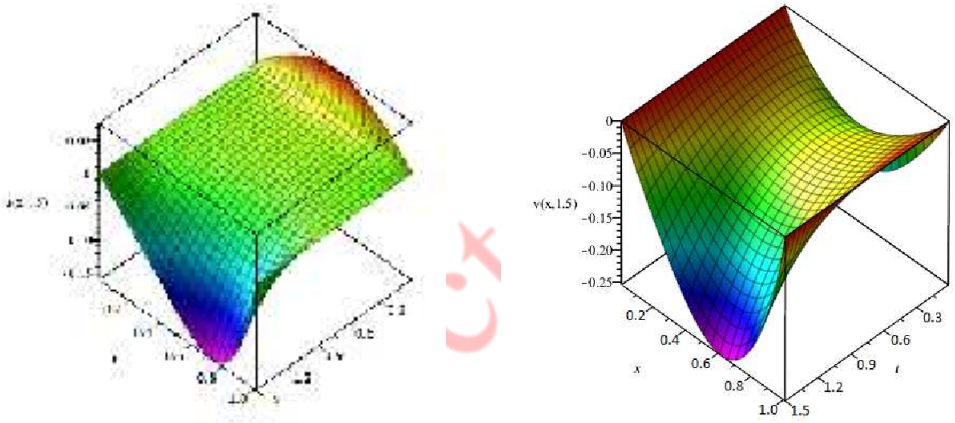

FIGURE 1. The graphs of the real (left) and the imaginary (right) parts of the approximate solution for $M = 12$, $\alpha = 0.25$, $\gamma = 1.8$, $\varepsilon = 0.15$, $\sigma = 3$ and $\tau = 0.01$ at $t = 1.5$ in Example 3.

Example 5.4. Consider

$$i\,{}^{c}D_{t}^{\alpha}\psi(x,y,t) + \frac{\partial^{\gamma}\psi(x,y,t)}{\partial|x|^{\gamma}} + \frac{\partial^{\gamma}\psi(x,y,t)}{\partial|y|^{\gamma}} + 2|\psi(x,y,t)|^{2}\psi(x,y,t) = f(x,y,t),$$

with the conditions

$$\begin{aligned}
\psi(x,y,0) &= 0,\\
\psi(0,y,t) &= 0,\\
\psi(1,y,t) &= 0,\\
\psi(x,0,t) &= 0,\\
\psi(x,1,t) &= 0,
\end{aligned}$$

where

$$f(x,y,t) = i\frac{120}{\Gamma(6-\alpha)}t^{5-\alpha}(1+i)\mathcal{A}(x)\mathcal{A}(y) + 4(1+i)t^{15}\mathcal{A}^3(x)\mathcal{A}^3(y)$$
$$- c_\gamma t^5(1+i)\mathcal{A}(y)\left[\frac{2}{\Gamma(3-\gamma)}\mathcal{B}(x,2-\gamma) - \frac{12}{\Gamma(4-\gamma)}\mathcal{B}(x,3-\gamma) + \frac{24}{\Gamma(5-\gamma)}\mathcal{B}(x,4-\gamma)\right]$$
$$- c_\gamma t^5(1+i)\mathcal{A}(x)\left[\frac{2}{\Gamma(3-\gamma)}\mathcal{B}(y,2-\gamma) - \frac{12}{\Gamma(4-\gamma)}\mathcal{B}(y,3-\gamma) + \frac{24}{\Gamma(5-\gamma)}\mathcal{B}(y,4-\gamma)\right],$$

in which $\mathcal{A}(.)$ and $\mathcal{B}(.)$ are defined as

$$\mathcal{A}(z) = z^2(1-z)^2, \tag{5.1}$$

and

$$\mathcal{B}(z,k) = z^k + (1-z)^k.$$

The exact solution is $\psi(x,t) = (1+i)t^5x^2(1-x)^2y^2(1-y)^2$.
We solved the problem by our technique with $M_1 = M_2 = M$. We list the E_∞ errors and $C-order$'s resulted by the present method with $\varepsilon = 0.1$, $\sigma = 1$ and $M = 9$ in Table 7. As the table shows, $C-order$ is approximately $4-\alpha$. In Table 8, the errors E_∞ and E_2 together with the condition numbers of matrices ϕ_X and ϕ_Y for different numbers of Gaussian RBFs are listed. The table confirms both the convergence of the method and the well-conditioning of our interpolation.

TABLE 7. The $C-orders$ and E_∞ errors for $\alpha = 0.3$ and $\gamma = 1.85$ using presented method, at $t = 1$ in Example 4.

	Real part		Imaginary part	
τ	E_∞	$C-order$	E_∞	$C-order$
$\frac{1}{8}$	4.62964×10^{-7}	–	4.00842×10^{-7}	–
$\frac{1}{16}$	4.10012×10^{-8}	3.50	3.56275×10^{-8}	3.49
$\frac{1}{32}$	3.43238×10^{-9}	3.58	2.98845×10^{-9}	3.58
$\frac{1}{64}$	2.78974×10^{-10}	3.62	2.43254×10^{-10}	3.62
$\frac{1}{128}$	2.22503×10^{-11}	3.65	1.95099×10^{-12}	3.64

TABLE 8. The comparison of E_∞ and E_2 errors and condition number for different values of M using presented method with $\alpha = 0.2$, $\gamma = 1.9$, $\tau = 0.025$ and $\varepsilon = 0.1$, $\sigma = 1$ at $t = 1$ in Example 4.

	Real part		Imaginary part			
M	E_∞	E_2	E_∞	E_2	$\kappa_\infty(\phi_X)$	$\kappa_\infty(\phi_Y)$
4	2.394723×10^{-3}	8.371867×10^{-3}	2.509691×10^{-3}	8.908535×10^{-3}	4.3014	4.3014
5	6.261892×10^{-6}	2.051060×10^{-5}	6.574005×10^{-6}	2.162577×10^{-5}	5.2903	5.2903
6	1.387267×10^{-6}	4.151272×10^{-6}	1.370691×10^{-6}	4.191423×10^{-6}	6.2861	6.2861
7	3.722687×10^{-9}	1.016861×10^{-8}	3.184190×10^{-9}	1.028350×10^{-8}	7.2853	7.2853
8	6.452195×10^{-10}	3.117526×10^{-9}	1.028044×10^{-9}	3.111826×10^{-9}	8.2866	8.2866

6. Conclusion

We developed the stable Gaussian RBF interpolation to solve nonlinear TSFSE. In this regard, we obtained the Riesz fractional derivative of the eigenfunction Gaussian interpolants, and by a method of lines, we converted the problem to a coupled system of fractional ODEs. To solve this system, we proposed a high order finite difference

scheme. We included four numerical examples to certify the efficiency of the method. Numerical experiments show that the condition number of ϕ_X is small and the accuracy of solutions are acceptable. We developed our technique for two-dimensional TSFSE. Our method gives a closed form approximate solution in each time step, and it can be extended for many types of time- and space-fractional PDEs.

References

[1] X. Antonie, Q. Tang, and J. Zhang, *On the numerical solution and dynamical laws of nonlinear fractional Shrödinger/Gross-Pitaevskii equations*, International journal of computer mathematics, *6-7* (2018), 1423–1443.

[2] M. D. Buhman, *Spectral convergence of multiquadratic interpolation*, Proc. Edinburg Math. Soc., *36* (1993), 319–333.

[3] J. X. Cao, C. P. Li, and Y. Q. Chen, *High-order approximation to Caputo derivatives and Caputo-type advection-diffusion equations (II)*, Fractional Calculus and Applied Analysis, *18*(3) (2015), 735-761.

[4] R. E. Carlson and T. A. Foley, *The parameter r^2 in multiquadratic interpolation*, Comput. Math. Appl., *21* (1991), 29–42.

[5] R. Cavoretto, G. E. Fasshauer, and M. McCourt, *An introduction to the Hilbert-Schmidt SVD using iterated Brownian bridge kernels*, Numer. Algorithms, *68*(2) (2015), 393-422.

[6] E. H. Dohaa, A. H. Bhrawy, and S. S. Ezz-Eldien, *A Chebyshev spectral method based on operational matrix for initial and boundary value problems of fractional order*, Computers and Mathematics with Applications, *62* (2011), 2364–2373.

[7] G. E. Fasshauer and M. J. MacCourt, *Stable evaluation of Gaussian radial basis function interpolants*, SIAM J. Sci. Comput., *34*(2) (2012), A737–A762.

[8] R. P. Feynman and A. R. Hibbs, *Quantum mechanics and path integrals*, McGraw-Hill, New York, NY, USA, 1965.

[9] B. Guo, Y. Han, and J. Xin, *Existence of the global smooth solution to the period boundary value problem of fractional nonlinear Schrödinger equation*, Applied Mathematics and Computation, *204*(1) (2008), 468–477.

[10] M. A. E. Herzallah and K. A. Gepreel, *Approximate solution to the time-space fractional cubic nonlinear Schrödinger equation*, Appl. Math. Model., *36* (2012), 5678–5685.

[11] J. Hu, J. Xin, and H. Lu, *The global solution for a class of systems of fractional nonlinear Schrödinger equations with periodic boundary condition*, Computers and Mathematics with Applications, *62*(3) (2011), 1510–1521.

[12] A. A. Kilbas, H. M. Srivastava, and J. J. Trujillo, *Theory and applications of fractional differential equations*, Elsevier, Amsterdam, 2006.

[13] M. Kirane, *Finite element method for time- space- fractional Schödinger equation*, Electronic Journal of Differential Equations,*166* (2017), 1–18.

[14] N. Laskin, *Fractional Schrdinger equation*, Phys. Rev. E, *66* (2002), 056108.

[15] N. Laskin, *Fractals and quantum mechanics*, Chaos, *10* (2000), 780–790,.

[16] Q. Liu, Y. T. Gu, P. Zhuang, F. Liu, and Y. F. Nie, *An implicit RBF meshless approach for time fractional diffusion equations*, Comput. Mech., *48*, (2011), 1–12.

[17] W. K. Liu and W. M. Han, *Reproducing kernel element method. Part I: Theoritical information*, Comput. Methods Appl. Mech. Engrg., *193* (2004), 933–951.

[18] N. Liu and W. Jiang, *A numerical method for solving the time fractional Schrödinger equation*, Adv Comput Math.,*44* (2018), 1235–1248.

[19] Q. Liu, F. Zeng, and Ch. Li, *Finite difference method for time-space-fractional Schödinger equation*, International Journal of Computer Mathematics, (2014), 1439–1451.

[20] J. M. Melenk and I. Babuska, *The partition of unity method: basic theory and applications*, Comput. Methods Appl. Mech. Engrg., *139* (1996), 289–314.

[21] M. Naber, *Time fractional Schrdinger equation*, J. Math. Phys., *45*(8) (2004), 3339–3352.

[22] M. Pazouki and R. Schaback, *Bases for kernel-based spaces*, Journal of Computational and Applied Mathematics,*236*(4) (2011), 575–588.

[23] C. Piret and E. Hanert, *A radial basis functions method for fractional diffusion equations*, J. Comput. Phys., *238* (2013), 71–81.
[24] I. Podlubny, *Fractional differential equations*, Academic Press, San Diego, 1999.
[25] A. Quarteroni, Riccardo Sacco, and Fausto Saleri, *Numerical mathematics*, Springer, 2000.
[26] J. Rashidinia, G. Fasshauer, and M. Khasi, *A stable method for the evaluation of Gaussian radial basis function solutions of interpolation and collocation problems*, Comput. Math. Appl., *72*(1) (2016), 178–193.
[27] J. Rashidinia and M. Khasi, *Stable Gaussian radial basis function method for solving Helmholtz equations*, Computational Methods for Differential Equations, *7*(1) (2019), 138–151.
[28] J. Rashidinia, M. Khasi, and G. E. Fasshauer, *A stable Gaussian radial basis function method for solving nonlinear unsteady convection-diffusion-reaction equations*, Computers and Mathematics with Applications, *75* (2018), 1831–1850.
[29] S. G. Samko, A. A. Kilbas, and O.I. Marichev, *Fractional integrals and derivatives: Theory and applications*, Gordon and Breach, New York, 1993.
[30] L. S. Schulman, *Techniques and applications of path integration*, John Wiley and Sons, New York, NY, USA, 1981.
[31] P. Wang and C. Huang, *An energy conservative difference scheme for the nonlinear fractional Schrödinger equations*, J. Comput. Phys., *293* (2015), 238–251.
[32] D. Wang, A. Xiao, and W. Yang, *Crank-Nicolson difference scheme for the coupled nonlinear Schrödinger equations with the Riesz space fractional derivative*, J. Comput. Phy., *242* (2013), 670–681.
[33] D. Wang, A. Xiao, and W. Yang, *Maximum-norm error analysis of a difference scheme for the space fractional CNLS*, Appl. Math. Comput., *257* (2015), 241–251.
[34] S. W. Wang and M. Y. Xu, *Generalized fractional Schrödinger equation with space-time fractional derivatives*, J. Math. Phys., *48* (2007), 043502.
[35] X. Zhao, Z. Z. Sun, and Z. P. Hao, *A fourth-order compact ADI scheme for two-dimensional nonlinear space fractional Schrödinger equation*, SIAM J. Sci. Comput., *36*(6) (2014), A2865–A2886.